

Mono- b signature as a probe of stop at the HL-LHC and HE-LHC

Tian-Peng Tang, Lei Wu, and Hang Zhou

Department of Physics and Institute of Theoretical Physics,

Nanjing Normal University, Nanjing, 210023, China

Abstract

Top-squarks (stop) play an important role in SUSY naturalness. The stop pair production is considered as the most effective way to search for stop at the LHC. However, the collider signature of stop pair production is usually characterized by $t\bar{t}$ plus missing transverse energy, which is also predicted in many other non-supersymmetric models. On the other hand, the single stop production via the electroweak interaction can provide some distinctive signatures, and thus will help to confirm the existence of the stop. In this paper, we investigate the observability of the mono- b events from the single stop production process $pp \rightarrow \tilde{t}_1 \tilde{\chi}_1^- \rightarrow b + \cancel{E}_T$ in a simplified MSSM framework where the higgsinos and stops are the only sparticles at the HL-LHC and HE-LHC. We find that the stop mass and the higgsino mass can be probed up to about 1600 GeV and 550 GeV at 5σ level at the HE-LHC with the integrated luminosity $\mathcal{L} = 15 \text{ ab}^{-1}$. We also present the 2σ exclusion limits of the stop mass at the HL-LHC and HE-LHC.

I. INTRODUCTION

With the Higgs boson discovered in 2012 [1, 2], the last piece of the puzzle of the Standard Model (SM) was found. This has made the SM a great success. However, the SM is in lack of the dark matter candidate and has the hierarchy problem. Therefore, it is widely believed that the new physics will emerge at the TeV scale, and stabilize the Higgs mass without fine tuning the theory parameters. Among these models, the low energy supersymmetry (SUSY) is one of the most promising extensions of the SM.

In supersymmetry, the top quark partners, namely stops, play a crucial role in canceling the quadratic divergence of the top quark loop, and thus protect the Higgs mass at the weak scale. In the minimum supersymmetric standard model (MSSM), the minimization conditions of the Higgs potential imply [3]:

$$\begin{aligned} \frac{M_Z^2}{2} &= \frac{(m_{H_d}^2 + \Sigma_d) - (m_{H_u}^2 + \Sigma_u) \tan^2 \beta}{\tan^2 \beta - 1} - \mu^2 \\ &\simeq -\mu^2 - (m_{H_u}^2 + \Sigma_u), \end{aligned} \quad (1)$$

where $m_{H_u}^2$ and $m_{H_d}^2$ are the weak scale soft SUSY breaking masses of the Higgs fields and μ is the higgsino mass parameter. $\tan \beta \equiv v_u/v_d$ is the ratio of vacuum expectation values of the two Higgs doublet fields H_u and H_d . Σ_u and Σ_d arise from the radiative corrections to the Higgs potential and the one-loop dominant contribution to Σ_u is given by [4]

$$\Sigma_u \sim \frac{3Y_t^2}{16\pi^2} \times m_{\tilde{t}_i}^2 \left(\log \frac{m_{\tilde{t}_i}^2}{Q^2} - 1 \right). \quad (2)$$

This indicates that only a small portion of the supersymmetric partners is closely related to the naturalness of the Higgs potential [5]. In order to obtain the value of M_Z naturally, each term in the right of Eq. (1) should be comparable in magnitude. Thus, if we now require 10% fine tuning, the higgsino mass μ should be around 100 – 200 GeV, which may be accessible by the monojet(-like) signature at the LHC [6]. In addition, the requirement of $\Sigma_u \sim M_Z^2/2$ leads to an upper bound on the stop mass $m_{\tilde{t}_{1,2}} \lesssim 1.5$ TeV [7]. Therefore, searching for the stops is a vital task to test SUSY naturalness [8–24].

During the LHC Run-1 and Run-2, the stops pair production have been extensively searched for by the ATLAS and CMS collaborations. The null results indicate that the stop mass should be heavier than several hundreds GeV [25, 26]. On the other hand, the stop can be singly produced through the associated production process $gb \rightarrow \tilde{t}_1 \tilde{\chi}_1^-$ (see

Fig. 1) via the electroweak interaction. Although the stop pair production is usually the most effective approach to search for the stop, its collider signature that has $t\bar{t}$ plus missing transverse energy in the final states is present in many other non-supersymmetric models, such as fermionic top partners. Therefore, the electroweak production of stop that carries orthogonal information is needed to further confirm the existence of the stop [27–30].

Besides the LHC, the High Luminosity LHC (HL-LHC) and High Energy LHC (HE-LHC) have been widely discussed. The former will run at a colliding energy $\sqrt{s} = 14$ TeV with the integrated luminosity of 3 ab^{-1} , while the latter will be designed to operate at a center of mass energy $\sqrt{s} = 27$ TeV with the integrated luminosity of 15 ab^{-1} over 20 years of operation. In this work, we investigate the single stop production process $pp \rightarrow \tilde{t}_1 \tilde{\chi}_1^-$ in a simplified framework where the higgsinos and stops are the only sparticles in the MSSM at the HL-LHC and HE-LHC. Such a scenario is favored by the natural SUSY and has been widely studied in [31–35]. Due to the higgsinos being nearly degenerate, their decay products are very soft so that they will mimic the missing energy at the LHC. Hence the single stop production $pp \rightarrow \tilde{t}_1 \tilde{\chi}_1^-$ will give two distinctive signatures, namely, the mono- t $t + \cancel{E}_T$ from $\tilde{t}_1 \rightarrow t \tilde{\chi}_{1,2}^0$ and the mono- b $b + \cancel{E}_T$ from $\tilde{t}_1 \rightarrow b \tilde{\chi}_1^+$. The sensitivity of the hadronic and leptonic mono- t events has been studied at the HL-LHC in Ref. [29]. We will focus on the mono- b analysis and explore its observability at the HL-LHC and HE-LHC.

This paper is organized as follows. In Sec. II, we calculate the cross section of the single stop electroweak production process $pp \rightarrow \tilde{t}_1 \tilde{\chi}_1^-$. Then in Sec. III, we perform Monte Carlo study of the mono- b signature from this single stop production at the HL-LHC and HE-LHC. Finally in Sec. IV, we draw our conclusions.

II. CALCULATION OF SINGLE STOP PRODUCTION

In the MSSM, the kinetic terms of top-squark are given by,

$$\mathcal{L} = \sum_{\tilde{t}} (\partial_\mu \tilde{t}_L^* \partial_\mu \tilde{t}_R) \begin{pmatrix} \partial^\mu \tilde{t}_L \\ \partial^\mu \tilde{t}_R \end{pmatrix} - (\tilde{t}_L^* \tilde{t}_R) M_{\tilde{t}}^2 \begin{pmatrix} \tilde{t}_L \\ \tilde{t}_R \end{pmatrix}, \quad (3)$$

with the stop mass matrix

$$M_{\tilde{t}}^2 = \begin{pmatrix} m_{\tilde{Q}_{3L}}^2 + m_t^2 + D_L^t & m_t X_t^\dagger \\ m_t X_t & m_{\tilde{U}_{3R}}^2 + m_t^2 + D_R^t \end{pmatrix}, \quad (4)$$

where

$$D_L^t = m_Z^2 \left(\frac{1}{2} - \frac{2}{3} \sin^2 \theta_W \right) \cos 2\beta, \quad D_R^t = \frac{2}{3} m_Z^2 \sin^2 \theta_W \cos 2\beta, \quad X_t = A_t - \mu \cot \beta. \quad (5)$$

Here $m_{\tilde{Q}_{3L}}$ and $m_{\tilde{U}_{3R}}$ are the soft SUSY-breaking mass parameters, and A_t is the trilinear coupling. μ is the higgsino mass parameter. The mass eigenstates \tilde{t}_1 and \tilde{t}_2 can be obtained by a unitary transformation,

$$\begin{pmatrix} \tilde{t}_1 \\ \tilde{t}_2 \end{pmatrix} = \begin{pmatrix} \cos \theta_{\tilde{t}} & \sin \theta_{\tilde{t}} \\ -\sin \theta_{\tilde{t}} & \cos \theta_{\tilde{t}} \end{pmatrix} \begin{pmatrix} \tilde{t}_L \\ \tilde{t}_R \end{pmatrix}, \quad (6)$$

where the mixing angle $\theta_{\tilde{t}}$ is given by $\sin 2\theta_{\tilde{t}} = \frac{2m_t X_t}{m_{\tilde{t}_1}^2 - m_{\tilde{t}_2}^2}$ and $\cos 2\theta_{\tilde{t}} = \frac{m_{\tilde{Q}_{3L}}^2 + D_L^t - m_{\tilde{U}_{3R}}^2 - D_R^t}{m_{\tilde{t}_1}^2 - m_{\tilde{t}_2}^2}$.

Besides, the mass matrix of the neutralinos $\tilde{\chi}_{1,2,3,4}^0$ in gauge-eigenstate basis $(\tilde{B}, \tilde{W}, \tilde{H}_d^0, \tilde{H}_u^0)$ is given by

$$M_{\chi^0} = \begin{pmatrix} M_1 & 0 & -\cos \beta \sin \theta_W m_Z & \sin \beta \sin \theta_W m_Z \\ 0 & M_2 & \cos \beta \cos \theta_W m_Z & \sin \beta \cos \theta_W m_Z \\ -\cos \beta \sin \theta_W m_Z & \cos \beta \cos \theta_W m_Z & 0 & -\mu \\ \sin \beta \sin \theta_W m_Z & -\sin \beta \cos \theta_W m_Z & -\mu & 0 \end{pmatrix} \quad (7)$$

where $M_{1,2}$ are soft-breaking mass parameters for bino and wino. The Eq. 7 can be diagonalized by a unitary 4×4 matrix N [36]. While the mass matrix of the charginos $\tilde{\chi}_{1,2}^\pm$ in the gauge-eigenstates basis $(\tilde{W}^+, \tilde{H}_u^+, \tilde{W}^-, \tilde{H}_d^-)$ is given by

$$M_{\chi^\pm} = \begin{pmatrix} 0 & X^T \\ X & 0 \end{pmatrix} \quad (8)$$

with

$$X = \begin{pmatrix} M_2 & \sqrt{2} s_\beta m_W \\ \sqrt{2} c_\beta m_W & \mu \end{pmatrix} \quad (9)$$

Here the mass matrix X can be diagonalized by two unitary 2×2 matrices U and V [36].

When $m_{U_{3R}} \ll m_{Q_{3L}}$ and $\mu \ll M_{1,2}$, the lighter stop \tilde{t}_1 is dominated by right-handed stop component and the electroweakinos $\tilde{\chi}_{1,2}^0$ and $\tilde{\chi}_1^\pm$ are higgsino-like. Then \tilde{t}_1 will mainly decay to $b\tilde{\chi}_1^+$ with the branching ratio of $\sim 50\%$. As a proof of concept, we focus on a simplified MSSM framework where the higgsinos and right-handed stop are the only sparticles in our following study.

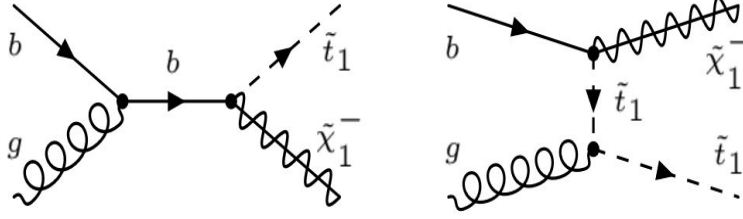


FIG. 1. Feynman diagrams of the single stop production process $pp \rightarrow \tilde{t}_1 \tilde{\chi}_1^-$ at the partonic level.

In Fig. 1, we show the Feynman diagrams of the single stop production process $g(p_a)b(p_b) \rightarrow \tilde{t}_1(p_1)\tilde{\chi}_1^-(p_2)$, whose amplitudes are given by,

$$i\mathcal{M}^{(s)} = g_s g_{eff} T_{\alpha\beta}^a \frac{\bar{u}(p_2)(\sin \theta_{eff} P_R + \cos \theta_{eff} P_L) \gamma_\mu u(p_b)}{(\not{p}_a + \not{p}_b) - m_b + i\epsilon} \epsilon^\mu(p_a), \quad (10)$$

$$i\mathcal{M}^{(t)} = g_s g_{eff} T_{\alpha\beta}^a \frac{\bar{u}(p_2)(\sin \theta_{eff} P_R + \cos \theta_{eff} P_L) u(p_b)}{(p_b - p_2)^2 - m_{\tilde{t}_1}^2 + i\epsilon} (p_{1\mu} - p_{b\mu} + p_{2\mu}) \epsilon^\mu(p_a), \quad (11)$$

with

$$\tan \theta_{eff} = \frac{y_b U_{12}^* \sin \theta_{\tilde{t}}}{-g_2 V_{11} \cos \theta_{\tilde{t}} + y_t V_{12} \sin \theta_{\tilde{t}}}. \quad (12)$$

Here y_b and y_t are the bottom and top quark Yukawa coupling, respectively. T_a are the Gellman-matrices. Then, we can have the partonic cross section in the center-of-mass frame at the leading order,

$$\frac{d\hat{\sigma}}{d\cos\theta} = \frac{|\vec{p}_1|}{16\pi\hat{s}^{3/2}} |\overline{\mathcal{M}}|^2. \quad (13)$$

where

$$|\vec{p}_1|^2 = \frac{(\hat{s} - m_{\tilde{t}_1}^2 - m_{\tilde{\chi}_1^-}^2)^2 - 4m_{\tilde{t}_1}^2 m_{\tilde{\chi}_1^-}^2}{4\hat{s}}, \quad \hat{s} = (p_a + p_b)^2. \quad (14)$$

Subsequently, the corresponding hadronic cross section can be obtained by convoluting the partonic cross section $\hat{\sigma}(gb \rightarrow \tilde{t}_1 \tilde{\chi}_1^-)$ with the parton distribution functions(PDFs), which is given by,

$$\sigma = \sum_{b,g} \int dx_1 f_{b/p}(x_1, \mu_F^2) \int dx_2 f_{g/p}(x_2, \mu_F^2) \hat{\sigma}_{gb \rightarrow \tilde{t}_1 \tilde{\chi}_1^-}(x_1 x_2 s). \quad (15)$$

where s is the squared pp centre-of-mass energy. The PDF $f_{b/p}$ is the number density of bottom quark carrying a fraction x_1 of the momentum of the first proton, and similarly with the PDF $f_{g/p}$ for the other proton. In our calculations, we use the CTEQ6L set with the factorization scale μ_F and renormalization scale μ_R chosen to be $\mu_R = \mu_F =$

m_Z . We calculate the leading order (LO) cross sections of the process $pp \rightarrow \tilde{t}_1 \tilde{t}_1^*$ with the MadGraph5_aMC@NLO [37] and include the NLO QCD corrections by applying a K factor of 1.4 [38–40]. The NLO QCD corrected cross sections of the process $pp \rightarrow \tilde{t}_1 \tilde{t}_1^*$ with the Prospino [41].

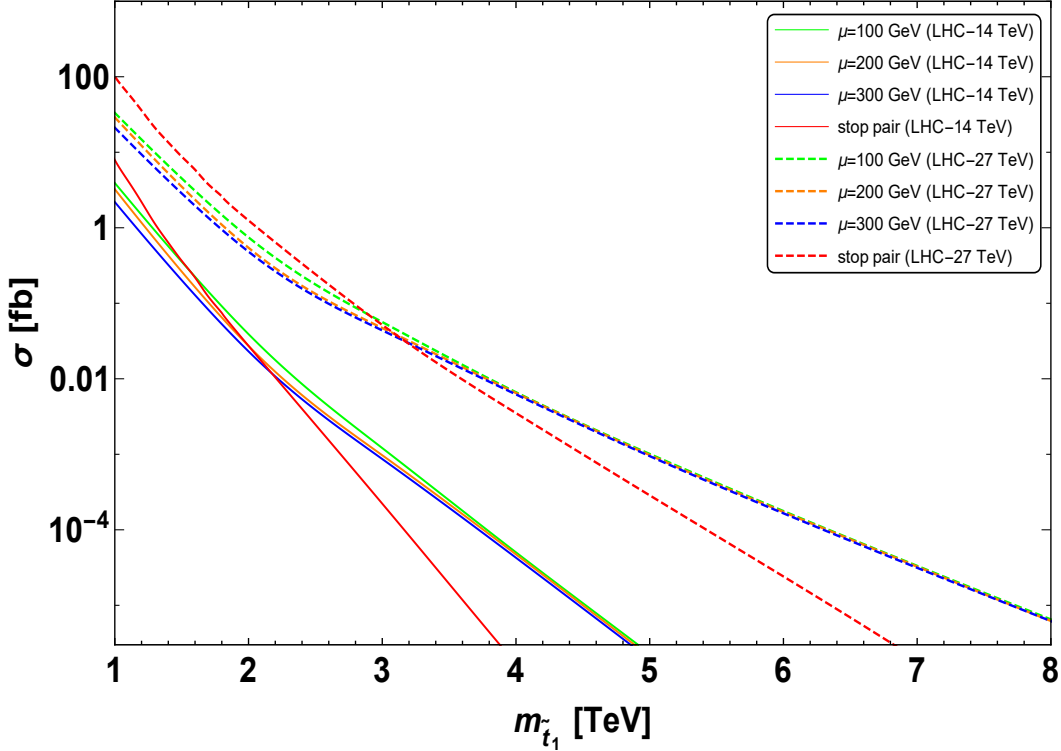


FIG. 2. The hadronic cross sections of the stop pair production process $pp \rightarrow \tilde{t}_1 \tilde{t}_1^*$ and the single stop production process $pp \rightarrow \tilde{t}_1 \tilde{\chi}_1^-$ at the 14 TeV and 27 TeV LHC. The contribution of the charge-conjugate process of the single stop production $pp \rightarrow \tilde{t}_1^* \tilde{\chi}_1^+$ is included.

In Fig. 2, we present the cross sections of the processes $pp \rightarrow \tilde{t}_1 \tilde{t}_1^*$ and $pp \rightarrow \tilde{t}_1 \tilde{\chi}_1^-$ at the LHC and HE-LHC. Since the electroweakinos can be still light [42], we take the higgsino mass parameter $\mu = 100, 200, 300$ GeV as an example. We vary the higgsino mass parameter μ and right-handed stop soft mass m_{U3} , and fix other soft supersymmetric masses at 1 TeV. We use the package SUSYHIT [43] to calculate masses, couplings and branching ratios of the sparticles. From Fig. 2, we can see that the cross section of the single stop production decreases slower than that of the stop pair production as stop becomes heavy. This is particular interesting for a stop in the TeV region. When the stop is heavier than about 2.2 TeV and 3.3 TeV, the single stop production may have a larger production rate than the stop pair production, due to the larger phase space.

III. OBSERVABILITY OF MONO-BOTTOM SIGNATURE AT THE HL/HE-LHC

Next, we investigate the mono- b signature for the single stop production, which is given by

$$pp \rightarrow \tilde{t}_1 \tilde{\chi}_1^- \rightarrow b \tilde{\chi}_1^+ \tilde{\chi}_1^- \rightarrow b + \cancel{E}_T. \quad (16)$$

It should be noted that the chargino $\tilde{\chi}_1^\pm$ in our scenario is treated as \cancel{E}_T because the mass difference between it and the LSP neutralino is small so that their decay products are very soft in the detectors. We use `MadGraph5_aMC@NLO` to generate the parton-level signal and background events. The parton shower and the detector simulations are implemented by `Pythia` [44] and `Delphes` [45] within the framework of `CheckMATE2` [46]. We use the anti- k_t jet clustering algorithm with a radius parameter $R = 0.4$ [47] and parameterize the b -jet tagging efficiency as in [48]. The largest SM background comes from the process $Z + jets$ because the light-flavor jets can be mis-tagged as b -jets. The subdominant backgrounds are the semi- and full-hadronic $t\bar{t}$ due to the mis-measurement of \cancel{E}_T from the undetected lepton and the limited jet energy resolution.

In Fig. 3, we show the normalized distributions of \cancel{E}_T (the transverse missing energy), $N(b)$ (the number of b jets), $p_T(b_1)$ (the transverse momentum of the leading b -jet) and H_{T3} (the scalar sum of the transverse momentum of the third to fifth jet) [49] for the signal and the background events at the 14 TeV LHC. The signal events has a larger \cancel{E}_T due to the massive $\tilde{\chi}_1^\pm$. The signal events have a harder $p_T(b_1)$ because the b -jet from the stop decay is boosted. The majority of $Z + jets$ and $t\bar{t}$ background events are distributed in the region of $\cancel{E}_T \lesssim 350$ GeV and $p_T(b_1) \lesssim 400$ GeV. Besides, the Z +jets events has the least b -jets in the final states. The $t\bar{t}$ background events can be separated from the signal events in the H_{T3} distribution since there are fewer hard jets in the signal events. Similarly, these distributions are also shown for the HE-LHC in Fig. 4, where the signal events have larger \cancel{E}_T and $p_T(b_1)$ than the background events.

In our analysis, we perform the event selections as followings:

- The events with any isolated leptons are rejected.
- We require at least two jets, and at least one b -jet with the leading b -jet $p_T(b_1) > 500$ GeV at the HL-LHC and $p_T(b_1) > 550$ GeV at the HE-LHC.

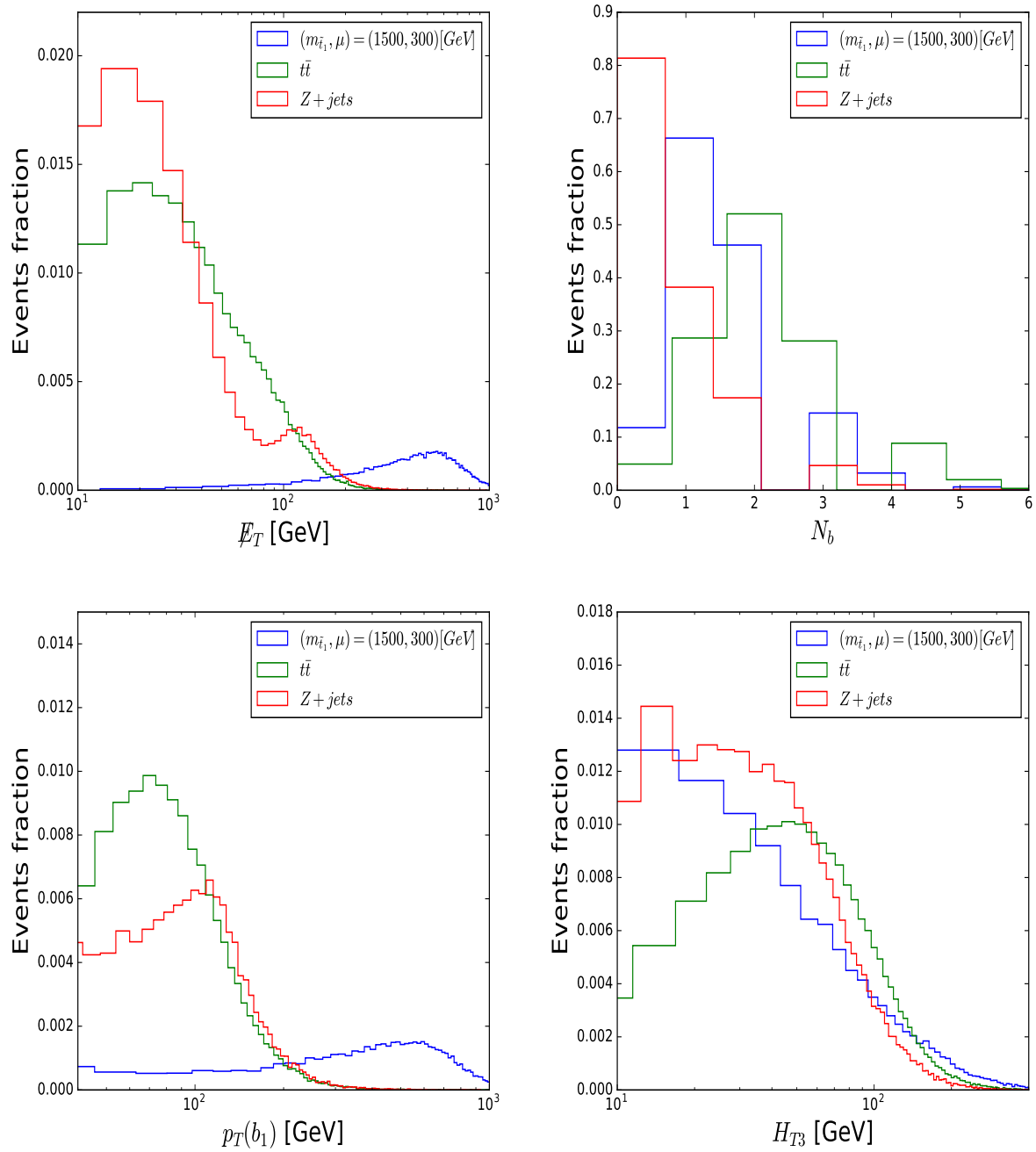


FIG. 3. The normalized distributions of \cancel{E}_T , $N(b)$, $p_T(b_1)$ and H_{T3} for the signal and the background events at 14 TeV LHC. The benchmark point is $m_{\tilde{t}_1} = 1500$ GeV and $\mu = 300$ GeV.

- We require $\cancel{E}_T > 450$ GeV at the HL-LHC and $\cancel{E}_T > 500$ GeV at the HE-LHC.
- $H_{T3} < 150$ GeV at the HL-LHC and $H_{T3} < 100$ GeV at the HE-LHC are required to further suppress the top pair background events.

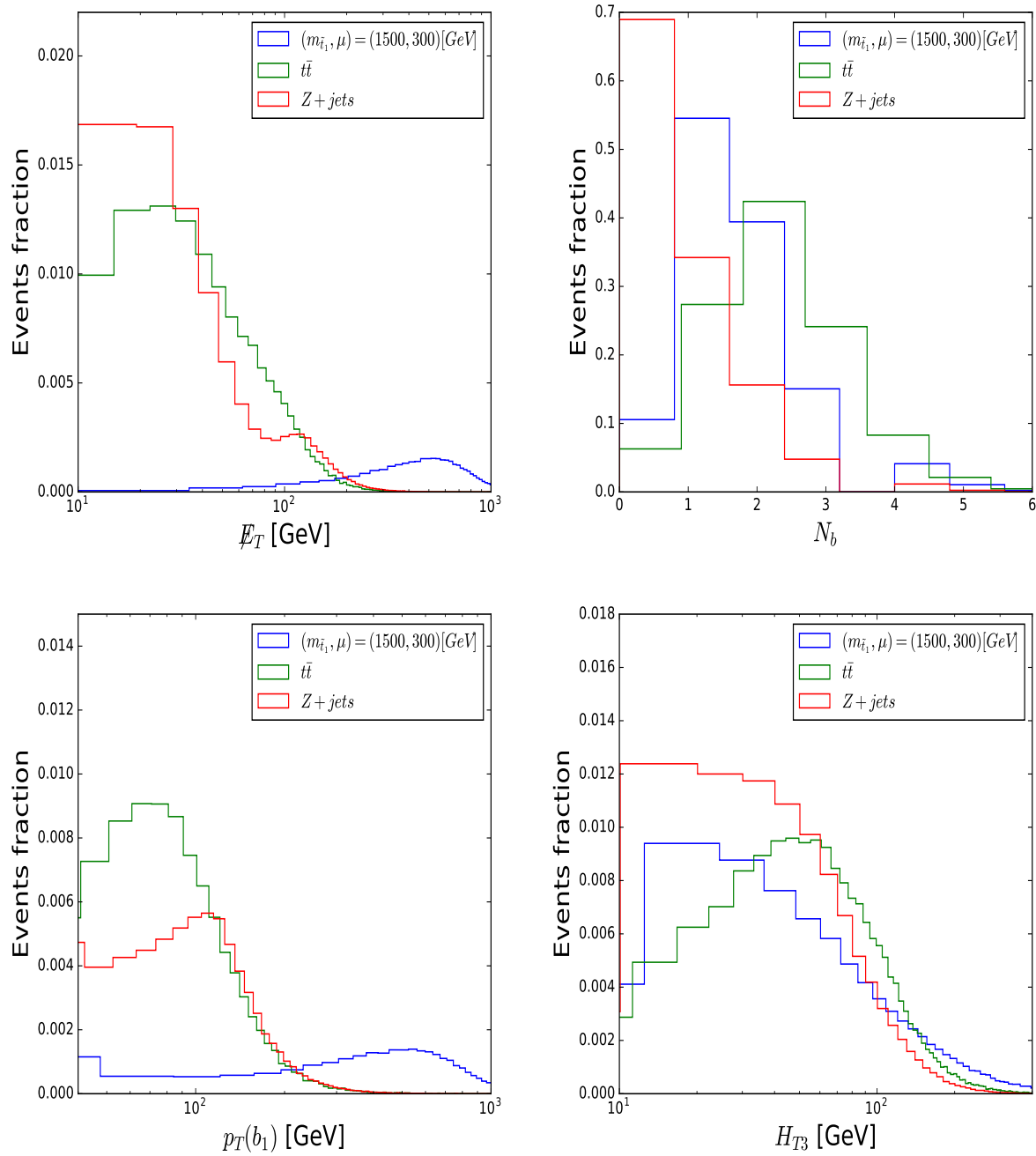


FIG. 4. Same as Fig. 3, but for the HE-LHC.

- A minimum azimuthal angle between any of the jets and the missing transverse momentum $\Delta\phi(j, \vec{p}_T) > 0.6$ is required to reduce the multi-jet background.

In Table I, we show the cut flow of the cross sections for the signal and backgrounds at the HL-LHC and HE-LHC. We can see that the large \cancel{E}_T cut will suppress $Z+jets$ and $t\bar{t}$

\sqrt{s}	HL-LHC			HE-LHC		
$m(\tilde{t}_1, \mu)$ [GeV]	(1500, 300)	Z +jets	$t\bar{t}$	(1500, 300)	Z +jets	$t\bar{t}$
Lepton veto	0.12	$5.83 \cdot 10^5$	$3.74 \cdot 10^5$	1.68	$1.68 \cdot 10^6$	$1.53 \cdot 10^6$
$N_j \geq 2$	0.11	$5.14 \cdot 10^5$	$3.72 \cdot 10^5$	1.56	$1.43 \cdot 10^6$	$1.51 \cdot 10^6$
$N_b \geq 1$	$8.02 \cdot 10^{-2}$	$1.12 \cdot 10^5$	$2.90 \cdot 10^5$	1.10	$3.16 \cdot 10^5$	$1.13 \cdot 10^6$
$\cancel{E}_T > 450$ [GeV]	$5.12 \cdot 10^{-2}$	39.53	49.59	—	—	—
$p_T(b_1) > 500$ [GeV]	$3.22 \cdot 10^{-2}$	7.72	11.31	—	—	—
$H_{T3} < 150$ [GeV]	$2.52 \cdot 10^{-2}$	5.83	4.78	—	—	—
$\cancel{E}_T > 500$ [GeV]	—	—	—	0.65	143.10	209.87
$p_T(b_1) > 550$ [GeV]	—	—	—	0.39	26.10	66.12
$H_{T3} < 100$ [GeV]	—	—	—	0.27	16.65	18.97
$\Delta\phi(j, \cancel{p}_T) > 0.6$	$1.90 \cdot 10^{-2}$	4.25	0.14	0.20	12.15	1.15

TABLE I. A cut flow analysis of the cross sections for the signal and backgrounds at the HL-LHC and HE-LHC. The cross sections are shown in unit of fb.

backgrounds by about $\mathcal{O}(10^3)$. The high $p_T(b_1)$ cut can further reduce the Z +jets. The H_{T3} and $\Delta\phi(j, \cancel{p}_T)$ cuts can remove the $t\bar{t}$ background effectively.

In Fig. 5, we present the contour plot of the statistical significance S/\sqrt{B} of the process $pp \rightarrow \tilde{t}_1 \tilde{\chi}_1^- \rightarrow b + \cancel{E}_t$ on the plane of stop mass $m_{\tilde{t}_1}$ versus the higgsino mass parameter μ at the HL-LHC and HE-LHC. We find that the stop mass $m_{\tilde{t}_1}$ and the higgsino mass μ can be excluded up to roughly 1200 GeV and 350 GeV at 2σ level at the HL-LHC, respectively. Such a bound will be extended by about 700 GeV for the stop mass and 400 GeV for the higgsino mass at the HE-LHC. Besides, the HE-LHC will be able to cover the stop with the mass $m_{\tilde{t}_1} \lesssim 1600$ GeV and the higgsinos with the mass $\mu \lesssim 550$ GeV at 5σ level.

IV. CONCLUSION

In this work, we studied the single stop production $pp \rightarrow \tilde{t}_1 \tilde{\chi}_1^-$ in a simplified MSSM framework where the higgsinos and right-handed stop are the only sparticles. Different from the conventional $t\bar{t} + \cancel{E}_T$ signature of the stop pair production, the single stop production predicts some distinctive signatures at the HL-LHC and HE-LHC, which will be useful to

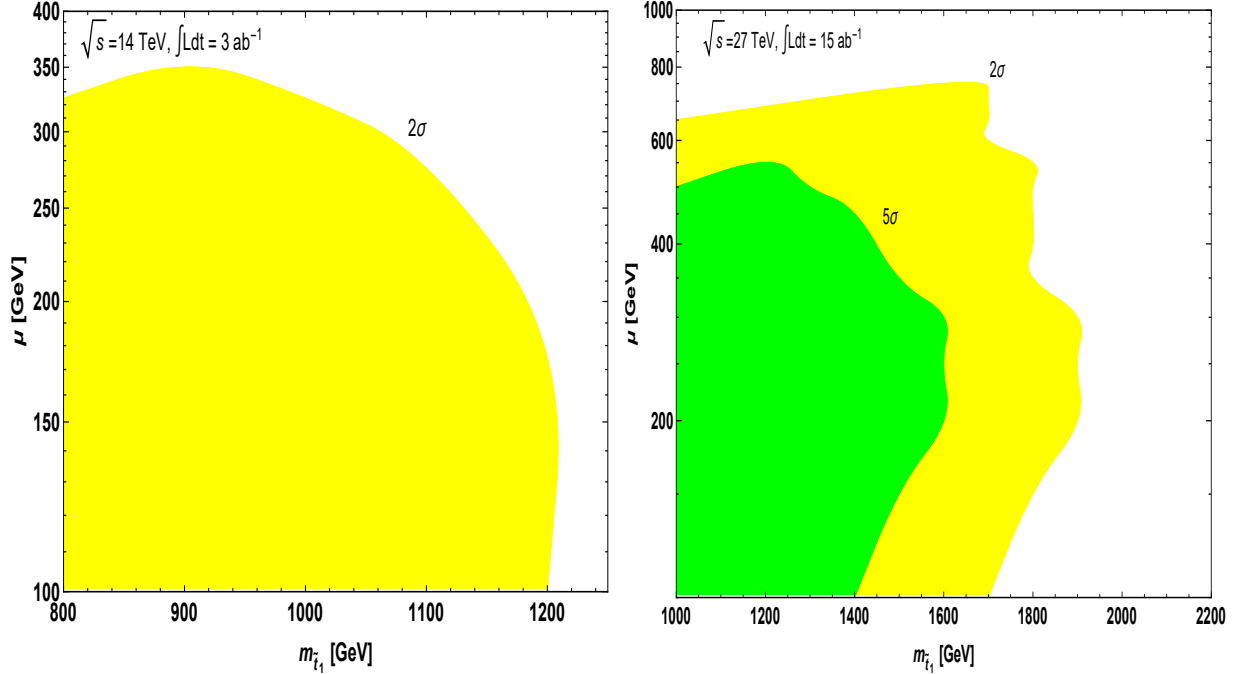


FIG. 5. The statistical significance S/\sqrt{B} of the process $pp \rightarrow \tilde{t}_1 \tilde{\chi}_1^- \rightarrow b + \cancel{E}_t$ on the plane of stop mass $m_{\tilde{t}_1}$ versus the higgsino mass parameter μ at the HL-LHC and HE-LHC.

examine the existence of the stop. We analyzed the sensitivity of the mono- b events from the single stop production process $pp \rightarrow \tilde{t}_1 \tilde{\chi}_1^- \rightarrow b \tilde{\chi}_1^+ \tilde{\chi}_1^- \rightarrow b + \cancel{E}_T$. We found that the mass reach of the stop can be up to about 1600 GeV at 5σ statistical significance at the HE-LHC with the integrated luminosity $\mathcal{L} = 15 \text{ ab}^{-1}$. In addition, if there was no significant excess in such a channel, the stop mass can be excluded up to about 1.2 TeV at the HL-LHC and 1.9 TeV at the HE-LHC.

ACKNOWLEDGEMENT

T. Tang would like to thank Murat Abdughani, Jie Ren and Jun Zhao for helpful discussions. This work was supported by the National Natural Science Foundation of China (NNSFC) under grant Nos. 11705093 and 11847208.

-
- [1] G. Aad *et al.* (ATLAS Collaboration), Phys. Lett. B **710**, 49 (2012).
 - [2] S. Chatrchyan *et al.* (CMS Collaboration), Phys. Lett. B **710**, 26 (2012).

- [3] R. Arnowitt and P. Nath, Phys. Rev. D **46**, 3981 (1992).
- [4] H. Baer, *et al.*, Phys. Rev. D **87**, 115028 (2013).
- [5] R. Barbieri and G. F. Giudice, Nucl. Phys. B **306**, 63 (1988).
- [6] C. Han, A. Kobakhidze, N. Liu, A. Saavedra, L. Wu and J. M. Yang, JHEP **1402**, 049 (2014) doi:10.1007/JHEP02(2014)049 [arXiv:1310.4274 [hep-ph]].
- [7] H. Baer, V. Barger, P. Huang, A. Mustafayev and X. Tata, Phys. Rev. Lett. **109**, 161802 (2012) doi:10.1103/PhysRevLett.109.161802 [arXiv:1207.3343 [hep-ph]].
- [8] L. J. Hall, D. Pinner and J. T. Ruderman, JHEP **1204**, 131 (2012).
- [9] M. Papucci, J. T. Ruderman and A. Weiler, JHEP **1209**, 035 (2012).
- [10] C. Brust, A. Katz, S. Lawrence and R. Sundrum, JHEP **1203**, 103 (2012).
- [11] J. Cao, C. Han, L. Wu, J. M. Yang and Y. Zhang, JHEP **1211**, 039 (2012) [arXiv:1206.3865 [hep-ph]].
- [12] G. Belanger, D. Ghosh, R. Godbole and S. Kulkarni, JHEP **1509**, 214 (2015);
- [13] C. Han, K. Hikasa, L. Wu, J. M. Yang and Y. Zhang, JHEP **1310**, 216 (2013).
- [14] M. Backovic, A. Mariotti and M. Spannowsky, JHEP **1506**, 122 (2015) [arXiv:1504.00927 [hep-ph]].
- [15] A. Kobakhidze, N. Liu, L. Wu and J. M. Yang, Phys. Rev. D **92**, 075008 (2015) [arXiv:1504.04390 [hep-ph]].
- [16] B. Dutta *et al.*, Phys. Rev. D **90**, 095022 (2014).
- [17] J. Fan, R. Krall, D. Pinner, M. Reece and J. T. Ruderman, JHEP **1607**, 016 (2016) [arXiv:1512.05781 [hep-ph]].
- [18] M. Schlaffer, M. Spannowsky and A. Weiler, Eur. Phys. J. C **76**, 457 (2016) [arXiv:1603.01638 [hep-ph]].
- [19] D. Goncalves, K. Sakurai and M. Takeuchi, Phys. Rev. D **94**, 075009 (2016) [arXiv:1604.03938 [hep-ph]].
- [20] D. Goncalves, K. Sakurai and M. Takeuchi, arXiv:1610.06179 [hep-ph].
- [21] L. Wu and H. Zhou, Phys. Lett. B **794**, 96 (2019) doi:10.1016/j.physletb.2019.05.033 [arXiv:1811.08573 [hep-ph]].
- [22] M. Abdughani, J. Ren, L. Wu and J. M. Yang, arXiv:1807.09088 [hep-ph].
- [23] G. H. Duan, L. Wu and R. Zheng, JHEP **1709**, 037 (2017) doi:10.1007/JHEP09(2017)037 [arXiv:1706.07562 [hep-ph]].

- [24] C. Han, J. Ren, L. Wu, J. M. Yang and M. Zhang, Eur. Phys. J. C **77**, no. 2, 93 (2017) doi:10.1140/epjc/s10052-017-4662-7 [arXiv:1609.02361 [hep-ph]].
- [25] M. Aaboud *et al.* [ATLAS Collaboration], JHEP **1712**, 085 (2017)
- [26] CMS Collaboration [CMS Collaboration], CMS-PAS-SUS-19-003.
- [27] D. Goncalves, D. Lopez-Val, K. Mawatari and T. Plehn, Phys. Rev. D **90**, 075007 (2014);
- [28] A. Ismail, R. Schwienhorst, J. S. Virzi and D. G. E. Walker, Phys. Rev. D **91**, 074002 (2015).
- [29] K. Hikasa, J. Li, L. Wu and J. M. Yang, Phys. Rev. D **93**, 035003 (2016).
- [30] G. H. Duan, K. i. Hikasa, L. Wu, J. M. Yang and M. Zhang, JHEP **1703**, 091 (2017) doi:10.1007/JHEP03(2017)091 [arXiv:1611.05211 [hep-ph]].
- [31] G. D. Kribs, A. Martin and A. Menon, Phys. Rev. D **88**, 035025 (2013).
- [32] K. Kowalska and E. M. Sessolo, Phys. Rev. D **88**, 075001 (2013).
- [33] A. Kobakhidze, N. Liu, L. Wu, J. M. Yang and M. Zhang, Phys. Lett. B **755**, 76 (2016).
- [34] M. Drees and J. S. Kim, Phys. Rev. D **93**, 095005 (2016).
- [35] H. Baer, V. Barger, N. Nagata and M. Savoy, Phys. Rev. D **95**, no. 5, 055012 (2017) doi:10.1103/PhysRevD.95.055012 [arXiv:1611.08511 [hep-ph]].
- [36] J. F. Gunion and H. E. Haber, Nucl. Phys. B **272**, 1 (1986).
- [37] J. Alwall *et al.*, JHEP **1407**, 079 (2014).
- [38] L. G. Jin, C. S. Li and J. J. Liu, Phys. Lett. B **561**, 135 (2003) doi:10.1016/S0370-2693(03)00422-2 [hep-ph/0307390].
- [39] L. G. Jin, C. S. Li and J. J. Liu, Eur. Phys. J. C **30**, 77 (2003) doi:10.1140/epjc/s2003-01261-x [hep-ph/0210362].
- [40] D. Goncalves, D. Lopez-Val, K. Mawatari and T. Plehn, Phys. Rev. D **90**, no. 7, 075007 (2014)
- [41] W. Beenakker, R. Hopker and M. Spira, hep-ph/9611232.
- [42] P. Athron *et al.* [GAMBIT Collaboration], Eur. Phys. J. C **79**, no. 5, 395 (2019) doi:10.1140/epjc/s10052-019-6837-x [arXiv:1809.02097 [hep-ph]].
- [43] A. Djouadi, M. M. Muhlleitner and M. Spira, Acta Phys. Polon. B **38**, 635 (2007)
- [44] T. Sjostrand, S. Mrenna and P. Z. Skands, JHEP **0605**, 026 (2006).
- [45] J. de Favereau *et al.* (DELPHES 3 Collaboration), JHEP **1402**, 057 (2014).
- [46] D. Dercks, N. Desai, J. S. Kim, K. Rolbiecki, J. Tattersall and T. Weber, Comput. Phys. Commun. **221** (2017) 383
- [47] M. Cacciari, G. P. Salam and G. Soyez, JHEP **0804**, 063 (2008).

- [48] CMS Collaboration, b-Jet Identification in the CMS Experiment, CMS-PAS-BTV-11-004.
- [49] M. Aaboud *et al.* [ATLAS Collaboration], JHEP **1711** (2017) 195